

Efimov effect in non-integer dimensions induced by an external field

E. Garrido^a, A.S. Jensen^b

^a*Instituto de Estructura de la Materia, IEM-CSIC, Serrano 123, E-28006 Madrid, Spain*

^b*Department of Physics and Astronomy, Aarhus University, DK-8000 Aarhus C, Denmark*

Abstract

The Efimov effect can be induced by means of an external deformed one-body field that effectively reduces the allowed spatial dimensions to less than three. To understand this new mechanism, conceptually and practically, we employ a formulation using non-integer dimension, which is equivalent to the strength of an external oscillator field. The effect most clearly appears when the crucial two-body systems are unbound in three, but bound in two, dimensions. We discuss energy variation, conditions for occurrence, and number of Efimov states, as functions of the dimension. We use practical examples from cold atom physics of ^{133}Cs - ^{133}Cs - ^{133}Cs , ^{87}Rb - ^{87}Rb - ^{87}Rb , ^{133}Cs - ^{133}Cs - ^6Li , and ^{87}Rb - ^{87}Rb - ^{39}K . Laboratory tests of the effect can be performed with two independent parameters, i.e. the external one-body field and the Feshbach two-body tuning. The scaling and (dis)appearance of these Efimov states occur precisely as already found in three dimensions.

Keywords: Efimov effect, confinement of quantum systems, d -dimensional calculations

1. Introduction

The Efimov effect was suggested theoretically about fifty years ago for three-body systems [1]. For the occurrence, at least two of the three pair-interactions must have nearly zero energy. Occurrence is optimized by having identical constituents, where only one two-body interaction is involved. However, although in principle possible, to find in nature two particles, identical or not, bound by zero energy would be very rare.

In cold atom physics this problem was overcome about 25 years ago with an original method, that is the technique of controlled tuning of the effective two-body interaction by coupling via a Feshbach resonance [2, 3, 4, 5]. Subsequently, properties and consequences of the Efimov effect have been extensively studied theoretically [6, 11, 10, 7, 8, 9] and also early established experimentally [12, 13, 14, 15, 16, 17, 18].

An important fact concerning the Efimov effect is that, whereas present in three dimensions (3D), is absent in two (2D) [22, 23, 19, 20, 21]. The reason is that in 3D a finite attraction is required for binding a two-body system, but in 2D an infinitesimal attraction is sufficient [24, 25]. These points emphasize the variation between dimensions, and in fact triggered previ-

ous investigations of dimensional transitions by different methods [26, 27, 28, 29]. In [30] it is shown how a two-species Fermi gas where one species is confined in a two- or one-dimensional space, while the other one is free in 3D, can lead, depending on the mass ratio, to systems showing the Efimov effect. This is the confinement-induced Efimov effect introduced in [31], although no details are given on the influence from continuous external squeezing. A short review of the effects of the confinement in mixed dimensions is given in [21].

A novel three-body method applicable to non-integer dimensions, d , was presented about two decades ago [6]. One spectacular prediction was that the Efimov effect is only possible in dimensions between 2.3 and 3.8. This d -method was recently implemented to investigate the confinement of two- and three-body systems [32, 33, 34, 35]. Practical calculations for non-integer dimensions are precisely as easy, or difficult, as in the usual 3D-space. The necessary relation to ordinary physics of integer-based dimensions is also available [32, 34]. The translation involves an external deformed field [36], which is shown to be equivalent to the non-integer dimensional treatment [35].

A detailed comparison of the actual wave function obtained introducing explicitly the external field and the deformed wave function extracted from the d -method is also given in [35] for different two-body potentials. It is

Email address: e.garrido@csic.es (E. Garrido)

shown how both wave functions are very much equivalent for both, well-bound and weakly bound, three-body systems. Thus, we can employ the simple method and interpret in terms of a deformed external one-body field.

The purpose of this letter is to demonstrate the power of the d -method by exhibiting a spectacular consequence of applying an external manageable [37] oscillator field to a three-body system. Assume the two-body attraction in 3D is too weak to bind. We then employ a squeezing one-body oscillator field on the z -direction, while leaving the x and y -coordinates untouched. The two-body systems are then forced to move towards 2D, where they at some point become bound through the unchanged two-body attractions. At this point of zero binding, the Efimov effect appears, which is at a non-integer dimension, or equivalently, at a certain strength of the external field.

Of course, the Feshbach resonance technique is still available, and the combination with an independent tuning of the deformed external field might prove convenient. The two independent parameters can be used to approach the optimal situation with three different subsystems at zero energy. This is not possible with only one parameter, neither Feshbach nor external field.

In this letter, we first describe the d -method and give enough details to allow calculations and estimates. We then present results for use on specific cold atom gases, where the Efimov effect can be manipulated to appear for non-integer dimensions.

2. The d -method

In Efimov's original formulation the key to understanding is that a long-distance effective attractive potential with an inverse-distance-square dependence arises for three particles with a strength more negative than a given critical value. The crucial potential term has the same form as a centrifugal barrier, which in ordinary three-dimensional space is positive. How and when this occurs is well established by some pathological conditions obeyed by the three constituent particles and their interactions. Although these occurrence conditions are special, they have been simulated in laboratories and a number of derived consequences experimentally tested.

To describe and understand in details it is convenient to adopt the formalism of the hyperspherical adiabatic expansion method, where the hyperradius, ρ , becomes the crucial length coordinate entering in the corresponding differential Schrödinger equation. The essential result, derived in many previous publications, e.g. [6],

takes the following form for each adiabatic channel:

$$\left(-\frac{\partial^2}{\partial \rho^2} + \frac{\lambda^{(d)}(\rho) + (d-1)^2 - \frac{1}{4}}{\rho^2} - \frac{2mE_{3b}^{(d)}}{\hbar^2} \right) f^{(d)}(\rho) = 0, \quad (1)$$

where d is the dimension parameter ($2 \leq d \leq 3$), $E_{3b}^{(d)}$ is the three-body energy in d dimensions, m is a normalization mass disappearing in all observable quantities, and $\lambda^{(d)}$ is the ρ -dependent eigenvalue from the angular Schrödinger (or Faddeev) equation. The reduced, $f^{(d)}$, and total, $F^{(d)}$, radial wave functions are related by

$$f^{(d)}(\rho) = \rho^{d-1/2} F^{(d)}(\rho). \quad (2)$$

Only the diagonal terms are included in Eq.(1), since the couplings between the adiabatic channels are unimportant as they vanish at the decisive large distances. Here we should remember that all such formula refer to one decoupled adiabatic channel.

The Efimov effect occurs for each channel for the particular dimension $d = d_E$ for which the numerator of the effective potential in Eq.(1) is, in the large- ρ limit, constant and less than $-1/4$. From Eq.(1) we see that this condition means that $\xi_{d_E}^2 < 0$, or $\xi_{d_E} = i|\xi_{d_E}|$, where we have defined

$$\xi_{d_E}^2 = \lambda_{\infty}^{(d_E)} + (d_E - 1)^2, \quad (3)$$

with $\lambda_{\infty}^{(d_E)} = \lambda^{(d_E)}(\rho = \infty)$.

The bound state solutions to Eq.(1) for constant $\lambda^{(d_E)} = \lambda_{\infty}^{(d_E)}$ are $f^{(d_E)}(\rho) \propto \sqrt{\kappa_{d_E} \rho} K_{i|\xi_{d_E}|}(\kappa_{d_E} \rho)$, with $\kappa_{d_E} = \sqrt{-2mE_{3b}^{(d_E)}/\hbar^2}$. The modified Bessel function of second kind, $K_{i|\xi_{d_E}|}$, decreases exponentially at large distances as it should for a bound state. For small distances we have instead $K_{i|\xi_{d_E}|} \propto \sin(|\xi_{d_E}| \ln(\kappa_{d_E} \rho))$.

It is important to keep in mind that in actual calculations the $\lambda^{(d_E)}$ -function is constant only over a ρ -interval limited by a scattering length, $|a_{d_E}^{av}|$, in practice finite, and defined as an average of the three d -dimensional two-body scattering lengths involved in the three-body system [10]. The condition $\xi_{d_E}^2 < 0$, or $\lambda_{\infty}^{(d_E)} < -(d_E - 1)^2$, and therefore the Efimov effect, requires that at least two of the two-body scattering lengths are numerically very large, which is equivalent to having close to zero energy in at least two of the two-body subsystems. For ρ larger than $|a_{d_E}^{av}|$ the λ -functions can no longer support bound states. The number, N_E , of Efimov states that can be held by a large, but finite, scattering length $a_{d_E}^{av}$, can be estimated by counting the number of nodes in $K_{i|\xi_{d_E}|}$ between the ground state size, ρ_0 , and $|a_{d_E}^{av}|$, that is [6]

$$N_E \approx \frac{|\xi_{d_E}|}{\pi} \ln \left(\frac{|a_{d_E}^{av}|}{\rho_0} \right). \quad (4)$$

The usual Efimov scaling for energies and root-mean-square (rms) radii still applies, which is [6]

$$\frac{E_n}{E_{n+1}} = \frac{\langle \rho^2 \rangle_{n+1}}{\langle \rho^2 \rangle_n} = e^{2\pi/|\xi_{dE}|}, \quad (5)$$

where n labels the different states in the Efimov series.

3. External field translation

The formulation in terms of the exceedingly intuitive dimension parameter, d , is very efficient and convenient for theoretical calculations. However, a relation to laboratory controlled observable variables is needed. This has recently become available in investigations where the particles are confined, say in the z -coordinate, by an external one-body oscillator field.

These calculations, where the deformed squeezing external oscillator potential with frequency ω_{ho} is included explicitly, are performed in a three-dimensional space, and they are related to the above d -results as shown in Ref.[35], which is:

$$\frac{\omega_{pp}}{\omega_{ho}} = \frac{2(d-2)}{(d-1)(3-d)}, \quad (6)$$

where ω_{pp} is the frequency of the equivalent two-body oscillator interaction that, when used in the three-body calculation, gives rise to the same rms radius $r_{2D} = \sqrt{2\hbar/(M\omega_{pp})}$, where M is the total mass, as the original potentials. In other words, in actual calculations with arbitrary two-body potentials, the computed value of r_{2D} permits to obtain ω_{pp} to be used in Eq.(6).

It was already shown in [6] that for s -waves and three identical bosons the appearance of the Efimov effect requires $d > 2.298$. This limit translates into $\omega_{ho} < 1.02\omega_{pp}$, which means that a squeezing frequency larger than $1.02\omega_{pp}$ cannot produce an Efimov effect for three identical bosons. For one light and two identical heavy particles the limit value can move up or down depending on the mass ratio, as shown in [33].

After a d -calculation, the equivalent deformed three-dimensional wave function is constructed by scaling down the z -direction by a factor, s , such that

$$\rho^2 \rightarrow \tilde{\rho}^2 = \rho_{\perp}^2 + \rho_z^2/s^2. \quad (7)$$

The constant scaling, s , is approximately given by [35]

$$\frac{1}{s^2} = \sqrt{1 + \frac{\omega_{ho}^2}{\omega_{pp}^2}} = \sqrt{1 + \left(\frac{(d-1)(3-d)}{2(d-2)} \right)^2}, \quad (8)$$

which connects the dimension d and the deformation, determined by the scale parameter s , of the actual three-dimensional wave function. We then replace $f^{(d)}(\rho)$ by

m_H/m_L	1/1 (3 ident.)	133/6	87/39
$E_{2D}^{(2bd)}$	-0.0987	-0.0987	-0.0987
a_{2D}	2.842	2.842	2.842
a_{3D}	-2.699	-2.699	-2.699
$E_{2D}^{(3gr)}$	-0.508	-0.341	-0.236
$E_{2D}^{(3*)}$	-0.101	-0.167	
$E_{2D}^{(3**)}$		-0.110	
$r_{2D}^{(3gr)}$	0.744	0.466	1.016
$r_{2D}^{(3*)}$	6.040	1.144	
$r_{2D}^{(3**)}$		2.545	

Table 1: We consider a three-body system made of two heavy identical particles with mass m_H and a light particle with mass m_L . The heavy-heavy interaction is zero. The heavy-light Gaussian interaction is with range, b , and strength $S = -0.943\hbar^2/(\mu b^2)$, where μ is the reduced mass of the system. For $m_H/m_L = 1$ the three particles and the corresponding interactions are identical. For $m_H/m_L=1, 133/6$, and $87/39$ we give two-body ground state energies, $E_{2D}^{(2bd)}$, and scattering lengths, a_{2D} , and a_{3D} in 2D and 3D. The lower part of the table shows, in 2D, the three-body energies and rms radii of the ground state and the existent excited states. Lengths are in units of b , and energies in units of $\hbar^2/(\mu b^2)$.

$f^{(d)}(\tilde{\rho})$, which, after the necessary renormalization, allows computations of any desired observable investigated in the laboratory from knowledge entirely from d -calculations, see [34, 35] for details.

4. Interactions and properties

Realistic numerical investigations need finite-range two-body potentials. We have chosen a potential such that the two-body systems are unbound in 3D, which will later permit to highlight the emergence of Efimov states for $2 \leq d \leq 3$. For our purpose any potential fulfilling these conditions could be used. The conclusions are independent of the specific potential shape.

For simplicity we choose a Gaussian radial shape, $S \exp(-r^2/b^2)$. This potential shape has been frequently used to investigate the Efimov effect, from the early days of three-body calculations [38], to much more recent works [39, 40]. Taking $\hbar^2/(\mu b^2)$ as energy unit, the properties of the two-body systems are mass-independent. In 2D the two-body systems have only one bound state, whose energy, $E_{2D}^{(2bd)}$, is given in the second row of Table 1. The following two rows give a_{2D} and a_{3D} , in units of b , which are the scattering lengths, a_d , for $d = 2$ and $d = 3$, respectively.

We consider three-body systems made of two identical heavy particles with mass m_H and a light particle with mass m_L . The interaction between the two heavy particles is put equal to zero, except for the mass ratio $m_H/m_L = 1$, where the three particles are considered

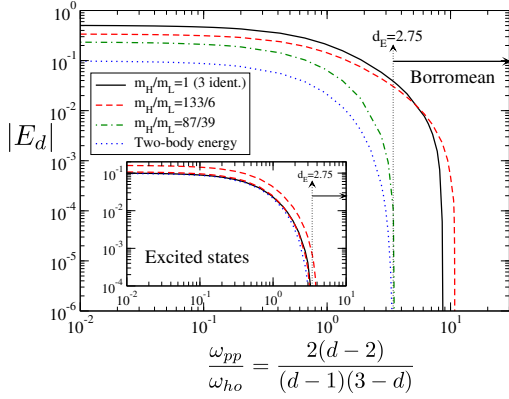


Figure 1: For the three-body states given in the lower part of Table 1, absolute value of the bound three-body energies, $|E_d|$ in units of $\hbar^2/(\mu b^2)$, as a function of the d -function in Eq.(6). The dotted blue curves is the absolute energy of the bound two-body state. The outer and inner panels show, respectively, the evolution of the ground state and the excited states. The black arrow indicates the region where the bound three-body states are borromean systems ($d > d_E$).

identical. As shown later, the asymmetric $m_H/m_L = 1$ case (one of the interactions equal to zero) is not particularly convenient for our purpose. The potential does not by choice bind the three-body systems in 3D, reflected by the moderately negative scattering length a_{3D} . In contrast, in the three cases shown in Table 1, the three-body system has one well bound ground state in 2D. Furthermore, also in 2D, the mass ratios $m_L/m_H = 1$ and $m_H/m_L = 133/6$ have one and two bound excited three-body states, respectively, see [41]. The corresponding energies are given in the lower part of Table 1 together with the root-mean-square radii for each of the states.

5. Energy variation

Starting from $d = 3$, when the dimension is decreased, i.e., when the system is progressively squeezed, the bound three-body states for each system appear from the continuum as shown in Fig. 1, where we show the binding energies as functions of the d -function in Eq.(6). The outer and inner panels show, respectively, the evolution of the ground and excited state energies for the different mass ratios. In both panels the dotted curve gives the evolution of the heavy-light two-body energy. The vertical dotted line at $d_E = 2.75$ marks the dimension below which the two-body system is bound. Therefore, all the three-body bound states located to the right of this vertical line have borromean character.

The overall behavior of the energy curves in Fig. 1 is similar for all the cases. When confining from 3D to 2D, moving from right to left in the figure, different bound

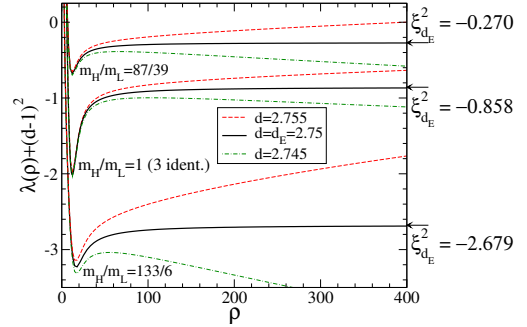


Figure 2: The functions $\lambda_n^{(d)} + (d-1)^2$ for the lowest diagonal potentials as functions of ρ for $d = d_E = 2.75$ (solid), $d = 2.755$ (dashed) and $d = 2.745$ (dot-dashed), for mass ratios $m_H/m_L = 1/1$ (3 identical particles), $133/6$, and $87/39$. The arrows indicate the asymptotic value of $\xi_{d_E}^2$ for $d = d_E$.

states appear, that is the ground states for $d = 2.89$, 2.91 , and 2.76 , for $m_H/m_L = 1$, $133/6$, and $87/39$, respectively. From this d -value, where the systems are borromean, an increase of the confinement (decrease of d) gives rise to a fast increase of the energy, which stabilizes following the same trend as the two-body energy. The behavior is similar for the excited states, shown in the inner panel, although the three-body energies are much closer to the two-body ones. In particular, the energy of the first excited state for $m_H/m_L = 1$ and the second excited state for $m_H/m_L = 133/6$, appearing both at $d = 2.76$, follow very closely the two-body energy. The first excited state for $m_H/m_L = 133/6$ appears at $d = 2.78$.

The dimension $d_E = 2.75$, corresponding to zero two-body energy, is the Efimov point, where infinitely many three-body bound states also emerge, and soon after disappear again. However, this d -value is rather arbitrary and the three coinciding Efimov points are only due to the choice of interactions. Increasing the two-body attraction, or equivalently $|a_{3D}|$, would move the corresponding Efimov point to the right on Fig 1. Eventually the well known Efimov condition would be reached in 3D with infinitely many states corresponding to zero two-body binding energy at $d = d_E = 3$. By weakening the attractive two-body potentials, the curves would move to the left towards 2D.

6. Asymptotic potentials

To understand the mechanism, we look at the effective potentials in Eq.(1). In Fig. 2 the solid curves show $\lambda^{(d)}(\rho) + (d-1)^2$ as functions of ρ , for the three coinciding Efimov points, $d = d_E = 2.75$, where $|a_d| = \infty$.

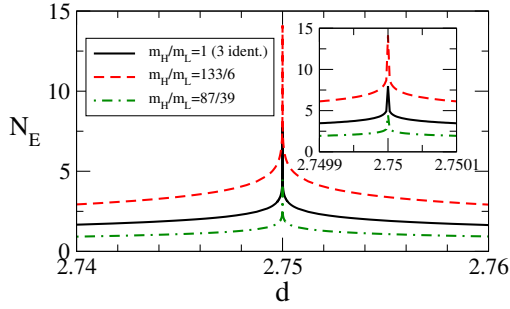


Figure 3: For $m_H/m_L = 1/1$ (solid), $133/6$ (dashed), $87/39$ (dot-dashed), estimated number, N_E , of bound excited states according to Eq.(4) with $\rho_0 = b$ as functions of d . The narrow peaks, which occur for the Efimov point of $d_E = 2.75$, are zoomed in the inset.

The functions are asymptotically constant, approaching the values $\xi_{d_E}^2 \approx -0.858, -2.679$, and -0.270 , for $m_H/m_L = 1/1, 133/6, 87/39$, respectively. These negative constants are criteria for occurrence of the Efimov effect in all the three cases.

The dashed and dot-dashed curves are the same functions for the neighboring d -values, $d = 2.755$ and $d = 2.745$, respectively. When $d > d_E$, as for $d = 2.755$, the $\lambda^{(d)}$ functions reproduce asymptotically the hyperspherical spectrum $K(K + 2d - 2)$ [6], which means that ξ_d^2 becomes positive for sufficiently large ρ . When $d < d_E$, as for $d = 2.745$, the $\lambda^{(d)}$ functions diverge parabolically to $-\infty$ [6], and the large negative asymptotic values prevent the appearance of bound states of large radii. Thus, there is no Efimov-like states for d outside a very narrow interval around d_E .

7. Number of Efimov states

As seen in Fig. 2, the variation with d of the effective potentials in Eq.(1) is very fast. The consequence is that the Efimov effect, i.e., the Efimov states, appear and disappear equally fast. We illustrate this in Fig. 3, where we show, as a function of d , the estimated number, N_E , of bound states across the Efimov point, as given in Eq.(4). We notice the extremely fast increase and decrease of the number of bound states, as highlighted in the inset. The tiny dimension interval, $2.7499 < d < 2.7501$, i.e., a tiny variation in the confinement, is enough to see essentially all the Efimov states appearing and disappearing. It is important to keep in mind that, as shown in Fig. 2, the strict Efimov conditions, i.e., asymptotic constant effective potentials and $\xi_{d_E}^2 < 0$, are only fulfilled for $d = d_E$. We also emphasize that these features are precisely as extreme as observed in the established Efimov scenario for $d = 3$.

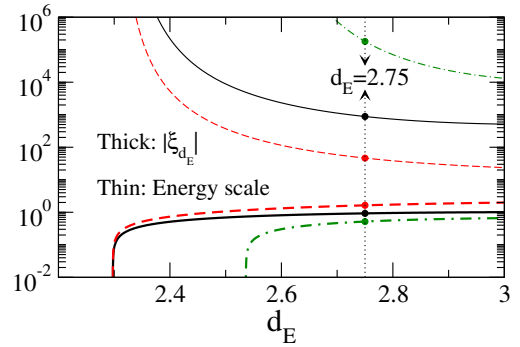


Figure 4: For $m_H/m_L = 1/1$ (solid), $133/6$ (dashed), $87/39$ (dot-dashed), value of $|\xi_{d_E}|$ as a function of d_E (thick) and the energy scale factor (thin) as given in Eq.(5).

In our calculations all the three Efimov points have arbitrarily been chosen to be $d = d_E = 2.75$. However, the properties of the Efimov states depend on the value of d_E . Fortunately, the large-distance constants, $\xi_{d_E}^2$, can be found independent of the interactions through a transcendental equation as explained in subsection 5.2.3 of Ref. [6]. As seen in Fig. 4 (thick curves), decreasing d_E produces decreasing $|\xi_{d_E}|$, which eventually becomes 0 for some $d_E = d_L$ limit value. The Efimov effect cannot occur for $d \leq d_L$, which for three identical bosons is $d_L = 2.298$, as already noted in [6]. For asymmetric systems, d_L oscillates depending on the mass ratio [33]. In particular, $d_L \approx 2.1$ for two non-interacting heavy and one light particles if $m_H/m_L \gg 1$, while d_L increases when m_H/m_L decreases. For $m_H/m_L = 133/6$ we get $d_L \approx 2.3$, as in the case of three identical particles, and $d_L \approx 2.54$ for $m_H/m_L = 87/39$.

In Fig. 4 we also show (thin curves) the energy scale factor, Eq.(5), which for given d_E decreases with increasing m_H/m_L ratio in the mass asymmetric case. This crucial fact allows easier numerical calculations of the Efimov states and facilitates as well experimental detection. This is evident in our case, $d_E = 2.75$, where the energy scale factors for $m_H/m_L = 133/6$ and $87/39$ are 46.5 and 180214, respectively, whereas we get 882.8 for the symmetric case of three identical particles ($m_L/m_H = 1$). This explains why the value of N_E in Fig. 3 is always above and below the other two curves for $m_H/m_L = 133/6$ and $m_H/m_L = 87/39$, respectively.

From the figure we can then conclude that, in the asymmetric case, the smaller the m_H/m_L ratio the closer $|\xi_{d_E}|$ to zero and, therefore, the larger the energy scale factor between the Efimov states. A reduction of the m_H/m_L ratio makes soon the Efimov states essentially unreachable both, theoretically and experimentally. As an example, for the asymmetric case with $m_H/m_L = 1$

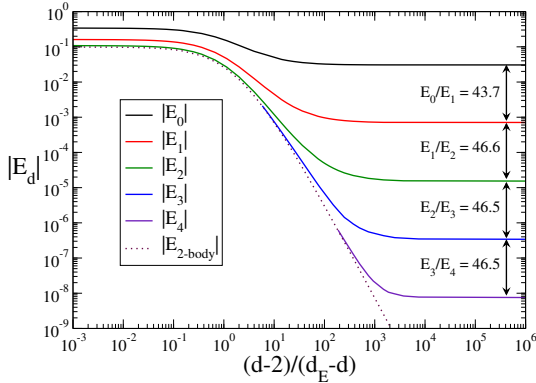


Figure 5: Absolute values of the bound three-body energies, $|E_d|$, in units of $\hbar^2/(\mu b^2)$, for the system of mass ratio, $133/6$, as functions of $(d-2)/(d_E-d)$, where $d_E = 2.75$ is the Efimov point for this interaction. The dotted curve correspond to the two-body binding energy.

the energy scales with a factor of about $2.5 \cdot 10^{10}$.

8. Efimov energies

The energies of the Efimov states appearing in the tiny d -interval above d_E towards the Efimov point are shown in Fig. 5 for the mass ratio $m_H/m_L = 133/6$. We show the lower side of the Efimov point, $d < d_E$, where the two identical two-body subsystems are always bound. In order to expand the small interval for visibility, we show the energies as functions of $(d-2)/(d_E-d)$. For comparison we also show the two-body binding energies in the figure (dotted curve).

The third and fourth excited states disappear along the two-body threshold, whereas the ground state and the two first excited states evolve as already shown by the dashed curves in Fig. 1. The energies of the five computed Efimov states for $d = d_E$ are, in units of $\hbar^2/(\mu b^2)$, $-3.050 \cdot 10^{-2}$, $-6.985 \cdot 10^{-4}$, $-1.498 \cdot 10^{-5}$, $-3.225 \cdot 10^{-7}$, and $-6.931 \cdot 10^{-9}$, respectively. The energy scale factors are then equal to 43.7, 46.6, 46.5, and 46.5, in very good agreement with the value (≈ 46.47) obtained from Eq.(5) for $\xi_{d_E}^2 = -2.679$ (see Fig.2).

In the higher side of the Efimov point, $d > d_E$, where the two identical two-body subsystems are unbound, the Efimov states disappear in the continuum, as shown in Fig. 1 for the two lowest states. Beyond d_E the energy of the different states drops rapidly, and eventually, for the interaction chosen in this work, the three-body states become unbound.

9. Conclusions

In this work we have explained a novel procedure that permits to obtain the Efimov conditions for a given three-body system. The tool is an external, directional squeezing, one-body potential. The usual external confining field, always present in cold atom experiments, must be deformed for our purpose, where a sufficiently strong deformation would squeeze the system continuously into two dimensions. The particles must then eventually adjust to a two-dimensional world, where even a weak two-body attraction supports a bound state.

Thus, for an interaction unable to bind the two-body system in three dimensions, at some intermediate deformation the two-body system must change from unbound to being bound. This Efimov point, with zero two-body binding energy, corresponds to an infinite scattering length, which leads to the infinite series of three-body Efimov states. As in three dimensions, this structure will emerge for any ground, or excited-state vanishing, two-body energy. The characteristic features are precisely the same as in three dimensions, and therefore open to the same type of tests.

The advantage now is that two independent controllable parameters are then available for tuning to the Efimov condition, that is Feshbach tuning and external field squeezing. This must in any case be more flexible than exploiting only one of these degree-of-freedom. It could be that an additional two-body subsystem can be made to contribute, perhaps the Feshbach tuning can be less precise, perhaps the Efimov scaling can be optimized to a denser spectrum with more opportunities, perhaps different systems can be studied, or perhaps applications on different problems present advantages.

We employed the recently formulated d -method, which is precisely as easy, or difficult, as an ordinary three-body calculation. It is equivalent to the brute force method of applying an external field, where one more three dimensional degree-of-freedom is required in more complicated calculations. The present results are obtained for identical bosons and for distinguishable particles. Additional applications are abundant, as for example more particles, different quantum symmetries, squeezing more than one dimension, or asymmetric squeeze of the dimensions.

Acknowledgments

This work has been partially supported by the Spanish Ministry of Science, Innovation and University MCIU/AEI/FEDER,UE (Spain) under Contract No. PGC2018-093636-B-I00.

References

References

- [1] V. M. Efimov, *Phys. Lett. B* 33, 563 (1970).
- [2] T. Köhler, K. Göral, and P. S. Julienne, *Rev. Mod. Phys.* 78, 1311 (2006).
- [3] I. Bloch, J. Dalibard, and W. Zwerger, *Rev. Mod. Phys.* 80, 885 (2008).
- [4] C. Chin, R. Grimm, P. Julienne, and E. Tiesinga, *Rev. Mod. Phys.* 82, 1225 (2010).
- [5] S. Deng, Z.-Y. Shi, P. Diao, Q. Yu, H. Zhai, R. Qi, and H. Wu, *Science* 353, 371 (2016).
- [6] E. Nielsen, D.V. Fedorov, A.S. Jensen, and E. Garrido, *Phys. Rep.* 347, 373 (2001).
- [7] E. Braaten and H.-W. Hammer, *Phys. Rep.* 428, 259 (2006).
- [8] E. Garrido, *Few-Body Syst.* 59, 17 (2018).
- [9] M. Mikkelsen, A. S. Jensen, D. V. Fedorov, and N. T. Zinner, *Journal of Physics B: Atomic, Molecular and Optical Physics* 48, 085301 (2015).
- [10] Fedorov D. V. and Jensen A. S. *Europhys. Lett.* 62, 336 (2003).
- [11] A.S. Jensen, K. Riisager, D.V. Fedorov, and E. Garrido, *Rev. Mod. Phys.* 76, 215 (2004).
- [12] T. Kraemer, M. Mark, P. Waldburger, J. G. Danzl, C. Chin, B. Engeser, A. D. Lange, K. Pilch, A. Jaakkola, H.-C. Nägerl, and R. Grimm, *Nature (London)* 440, 315 (2006).
- [13] M. Zaccanti, B. Deissler, C. D’Errico, M. Fattori, M. Jonas-Lasinio, S. Müller, G. Roati, M. Inguscio, and G. Modugno, *Nature Phys.* 5, 586 (2009).
- [14] S. E. Pollack, D. Dries, and R. G. Hulet, *Science* 326, 1683 (2009).
- [15] N. Gross, Z. Shotan, S. Kokkelmans, and L. Khaykovich, *Phys. Rev. Lett.* 103, 163202 (2009). *Phys. Rev. Lett.* 105, 103203 (2010).
- [16] J. H. Huckans, J. R. Williams, E. L. Hazlett, R. W. Stites, and K. M. O’Hara, *Phys. Rev. Lett.* 102, 165302 (2009).
- [17] T. B. Ottenstein, T. Lompe, M. Kohlen, A. N. Wenz, and S. Jochim, *Phys. Rev. Lett.* 101, 203202 (2008).
- [18] A. N. Wenz, T. Lompe, T. B. Ottenstein, F. Serwane, G. Zürn, and S. Jochim, *Phys. Rev. A* 80, 040702(R) (2009).
- [19] E. Nielsen, D.V. Fedorov, and A.S. Jensen, *Phys. Rev. A* 56, 3287 (1997).
- [20] A. G. Volosniev, D.V. Fedorov, A.S. Jensen, N.T. Zinner, *Eur. Phys. J. D* 67, 95 (2013).
- [21] P. Naidon and S. Endo, *Rep. Prog. Phys.* 80, 056001 (2017).
- [22] L.W. Bruch and J.A. Tjon, *Phys. Rev. A* 19, 425 (1979).
- [23] T.K. Lim and B. Shimer, *Z. Phys. A* 297, 185 (1980).
- [24] B. Simon, *Ann. Phys.* 97, 279 (1976).
- [25] A. G. Volosniev, D. V. Fedorov, A. S. Jensen, N. T. Zinner, *Phys. Rev. Lett.* 106, 250401 (2011).
- [26] J. Levinsen, P. Massignan, and M.M. Parish, *Phys. Rev. X* 4, 031020 (2014).
- [27] M.T. Yamashita, F.F. Bellotti, T. Frederico, D.V. Fedorov, A.S. Jensen, N. T. Zinner, *J. Phys. B: At. Mol. Opt. Phys.* 48, 025302 (2015).
- [28] J.H. Sandoval, F.F. Bellotti, A.S. Jensen, and M.T. Yamashita, *J. Phys. B: At. Mol. Opt. Phys.* 51, 065004 (2018).
- [29] D.S. Rosa, T. Frederico, G. Krein, and M.T. Yamashita, *Phys. Rev. A* 97, 050701(R) (2018).
- [30] Y. Nishida and S. Tan, *Phys. Rev. Lett.* 101, 170401 (2008).
- [31] Y. Nishida and S. Tan, *Phys. Rev. A* 79, 060701(R) (2009).
- [32] E. Garrido, A.S. Jensen, and R. Álvarez-Rodríguez, *Phys. Lett. A* 383, 2021 (2019).
- [33] E. R. Christensen, A.S. Jensen, and E. Garrido, *Few-Body Syst* 59, 136 (2018).
- [34] E. Garrido and A.S. Jensen, *Phys. Rev. Research* 1, 023009 (2019).
- [35] E. Garrido and A.S. Jensen, *Phys. Rev. Research* 2, 033261 (2020).
- [36] F. S. Møller, D. V. Fedorov, A. S. Jensen, N. T. Zinner, *J. Phys. B: At. Mol. Opt. Phys.* 52, 145102 (2019).
- [37] J.R. Armstrong, A.G. Volosniev, D.V. Fedorov, A.S. Jensen, and N.T. Zinner, *J. Phys. A: Math. Theor.* 48, 085301 (2015).
- [38] D.V. Fedorov, A.S. Jensen, and K. Riisager, *Phys. Rev. Lett.* 73, 2817 (1994).
- [39] A. Kievsky and M. Gattobigio, *Phys. Rev. A* 87, 052719 (2013).
- [40] L. Happ, M. Zimmermann, S.I. Betelu, W.P. Schleich, and M.A. Efremov, *Phys. Rev. A* 100, 012709 (2019).
- [41] F. F. Bellotti, T. Frederico, M. T. Yamashita, D. V. Fedorov, A. S. Jensen, N. T. Zinner, *Phys. Rev.* 85, 025601 (2012)